ELSEVIER

Wear 211 (1997) 44–53

WEAR

Towards a deeper understanding of wear and friction on the atomic scale—a molecular dynamics analysis

Liangchi Zhang *, Hiroaki Tanaka

Department of Mechanical and Mechatronic Engineering, The University of Sydney, Sydney, NSW 2006, Australia

Received 31 December 1996

Abstract

This study aims to gain an in-depth understanding of the mechanisms of wear and friction on the atomic scale through the investigation of a typical diamond–copper sliding system with the aid of molecular dynamics analysis. The study revealed that there generally exist four distinct regimes of deformation, i.e. the no-wear regime, adhering regime, ploughing regime and cutting regime. The transition between these regimes is governed by key sliding parameters such as indentation depth, sliding speed and surface lubrication conditions. The no-wear regime exists for a wide range of indentation depths and thus a no-wear design of practical sliding systems is possible even under chemically clean conditions. In the cutting regime, the frictional behaviour of the system follows a proportional law. In all the other regimes, however, the variation of the frictional force is complex and cannot be described by a simple formula. The study also pointed out that on the atomic scale the slip lines generated by dislocation motion are very different from those predicted by the slip-line theory of plasticity. A new theory needs to be developed to bridge the gap between atomic and micro analyses. © 1997 Elsevier Science S.A.

Keywords: Mechanism; Atomic scale; Molecular dynamics; Sliding; Diamond–copper

1. Introduction

A full understanding of wear and friction on the atomic scale is of fundamental importance to the development of nanotechnology. Immediate examples in which atomic wear and friction play a central role are the optimal design, fabrication and operation of devices with atomic resolution, such as micro-machines and high-density magnetic recording systems.

An experimental observation of atomic scale friction using an atomic force microscope was reported by a research group at IBM [1]. The friction coefficient between a tungsten tip of radius 300 nm and a basal plane of a graphite grain was found to be 0.012 at a normal load of 10 μN. Another interesting result was reported in Japan [2]. When sliding a tungsten tip of radius 10 μm on a carbon sputtered surface, a frictional force of about 1 μN at zero normal force was measured, indicating an infinite friction coefficient. In the meantime, theoretical studies using either molecular dynamics simulation or first-principle calculations [3–7] have also been carried out and showed that the friction coefficient could vary significantly, from 0.01 to 0.07, under different sliding conditions. Belak and Stowers [8] studied the indentation and scraping of a copper monocrystal by a rigid diamond tip using the molecular dynamics simulation. While focusing mainly on some issues of indentation with an observation of dislocation initiation, they also simulated cutting under a specific condition and observed that the friction coefficient was about 1.0. However, the mechanisms of friction and wear and the effect of deformation, sliding conditions and dislocation motions were not studied.

More systematic research was conducted recently by Homola [9], who proposed the concept of interfacial sliding to describe the sliding of two perfect, molecularly smooth and undamaged mica surfaces. Mechanisms of wear were also addressed. The investigation demonstrated that the Bowden–Tabor formula [10], which states that the frictional force is proportional to the real molecular contact area, could well describe the frictional behaviour during atomic sliding. In fact, the importance of the atomic contact area to atomic friction is not difficult to understand if the JKR theory [11] is recalled. This theory, while considering the effect of surface energy in its analysis, has implicitly indicated that the real contact area must be of great concern to sliding loads on the atomic scale.

In short, studies so far have been restrained either by the conventional definition of friction coefficient or by the limited examination of the effect of sliding conditions. Investigations

* Corresponding author.

PII S0043-1648(97)00073-2

into the mechanisms of wear during atomic sliding are still lacking. A general figure of the origin of friction and wear on the atomic scale has not been constructed. The present study aims to discuss these problems in detail.

2. Modelling

2.1. Molecular dynamics analysis

On the atomic scale, a solid material can no longer be viewed as a continuum. Thus conventional continuum mechanics is difficult to apply. On the other hand, the motion of individual atoms becomes dominant. In this study, therefore, we use the molecular dynamics (MD) method to analyse the deformation of an atomic lattice caused by sliding. [1]

Let us consider an atomically smooth diamond asperity sliding on an atomically smooth surface of a copper monocrystal in its (111) plane (see Fig. 1). The variables of interest are the sliding speed V, indentation depth d, degree of surface lubrication or contamination and the tip radius of asperity R which is the radius of the envelope of centres of the surface atoms. The environmental temperature of the sliding system is 293 K and the asperity rake angle is $-60°$.

The definition of indentation depth in the atomic sliding analysis needs to be clarified specifically. In any conventional study of sliding, the indentation depth of a hard asperity is the penetration depth of the asperity tip measured from the surface of the soft material. On the atomic scale, however, a definite surface does not exist because nuclei are surrounded by electron clouds. To resolve this problem conveniently, we assume that the surfaces of the diamond asperity and copper workpiece are defined by the envelopes at the theoretical radii of their surface atoms, respectively. In this way, the indentation depth d, defined in Fig. 1, becomes consistent with the conventional definition. In addition, we assume that d keeps constant in a sliding process, which implies that the sliding system has an infinite loop stiffness.

There are two special types of atoms in the MD modelling, as shown in Fig. 1. The thermostat atoms are arranged to ensure that the heat generated during sliding can conduct out of the control volume properly. The boundary atoms are fixed to the space to eliminate the rigid body motion of the copper specimen. As usual, the velocities of atoms in the initial configuration of the model follow the Maxwell distribution.

The interactions between an atom i and all the other atoms are governed by their net interaction potential ϕ, which is determined by experiment. The interaction between two atoms could be repulsive or attractive, depending on the interatomic separation r, as shown in Fig. 2, where r_0 is the equilibrium separation at which ϕ minimizes. The interaction is

[1] The MD analysis has been found a powerful tool for understanding the deformation mechanisms of materials on the atomic and nanometre scales [12–16]. To carry out a reliable MD analysis, however, some key factors that have often been overlooked must be addressed carefully. A detailed discussion on the issues of reliable MD modelling can be found in Ref. [16].

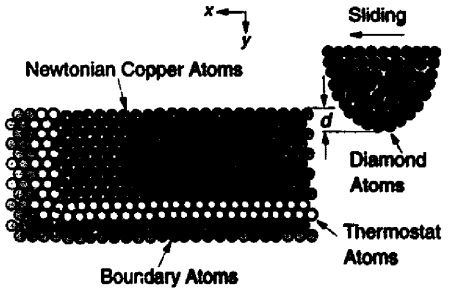

Fig. 1. Schematic model of a diamond–copper atomic sliding system in the (111) plane of a copper monocrystal. The sliding direction is [110].

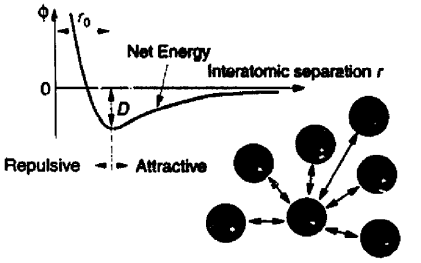

Fig. 2. Interatomic potential and interactions between atom pairs.

attractive when $r > r_0$ but becomes repulsive when $r < r_0$. In this study, we propose the following *modified Morse potential* to describe the interactions between copper and copper and between copper and diamond atoms. In the model shown in Fig. 1, if the separation between atoms i and j is r_{ij}, the modified Morse potential can be written as

$$\phi(r_{ij}) = \lambda_1 D\{\exp\{-2\lambda_2\alpha(r_{ij}-r_0)\} - 2\exp\{\lambda_2\alpha(r_{ij}-r_0)\}\} \quad (1)$$

where D and α are material constants listed in Table 1. The physical meaning of D is the cohesive energy between the two atoms. λ_1 and λ_2 are non-dimensional parameters indicating the cohesive strength change between the atom pair i–j. For copper–copper atom pairs, $\lambda_1 = \lambda_2 = 1$, hence Eq. (1) becomes identical to the standard Morse potential. For copper–diamond atom pairs, however, λ_1 takes a value in the interval $(0,1]$ whilst $\lambda_2 \geq 1$. This is because an application of lubrication or contamination on the diamond–copper interface weakens the cohesive strength between copper and diamond atoms. Hence the effect of surface lubrication or contamination on the friction and wear can be qualitatively investigated by varying λ_1 in $(0,1]$ and ignoring the detailed

Table 1
Parameters in the standard Morse potential

Parameter	Cu–Cu	Cu–C
D (eV)	0.342	0.087
α (nm^{-1})	13.59	51.40
r_0 (nm)	0.287	0.205

effects of lubricant or contaminant atoms, such as chemical effects. However, when λ_1 varies in (0,1], the potential curve between a pair of copper–diamond atoms will distort towards the negative direction of r. Bearing in mind that the atomic distance between any copper and diamond atoms increases, rather than decreases, when a lubricant or contaminant atom appears to separate them from direct contact, the potential curve should distort towards the positive direction of r. Hence λ_2 in Eq. (1) must be larger than unity. In the present analysis, we determine λ_2, when λ_1 changes, by keeping the spring constant of a copper–diamond atomic pair unchanged [2]. Obviously, $\lambda_1 = \lambda_2 = 1$ stands for a chemically clean environment.

With the above potential function available, the forces on atom i owing to the interaction of all the other atoms can be calculated by

$$\boldsymbol{F}_i = -\sum_{j=1, j\neq i}^{N} \nabla_i \phi(r_{ij}) \tag{2}$$

where N is the total number of atoms in the model [3], including thermostat, boundary and diamond atoms. Consequently, the motion of all the Newtonian atoms in the control volume, including their instant position and velocity vectors, can be obtained by following the standard procedures of molecular dynamics analysis [12,16].

In principle, an asperity is three-dimensional and thus a three-dimensional MD analysis would be more appropriate. However, we found, based on a careful comparison [15], that the two-dimensional model can lead to accurate enough results in terms of the variations of temperature and sliding forces, and easier characterization of deformation. We will therefore focus on the two-dimensional analysis in this study.

2.2. Dislocation analysis

When an instant configuration of the copper atomic lattice during sliding is obtained by the molecular dynamics analysis, the distribution of dislocations in the deformed lattice can be determined by the standard dislocation analysis [17]. Fig. 3 shows an example of identifying edge dislocations when two extra half-planes of atoms (dark atoms) appear in the deformed atomic lattice. The Burgers vector can be obtained by application of the Burgers circuit. Since we are carrying out a two-dimensional molecular dynamics simulation, we can only study edge dislocations [15]. For convenience, however, we call them dislocations throughout the paper.

It should be pointed out that the above method is convenient for discrete dislocations with lower density. If the number of dislocations in an area is very large, the determination of dislocations will become extremely time consuming.

[2] This means that when λ_1 is given, λ_2 is determined by $(\lambda_1 D)-(\lambda_2 a)^2 = Da^2$, which gives rise to $\lambda_2 = \lambda_1^{-1/2}$.

[3] In this study, $12\,000 \leq N \leq 15\,000$ is used in conjunction with the technique of moving control volume [16].

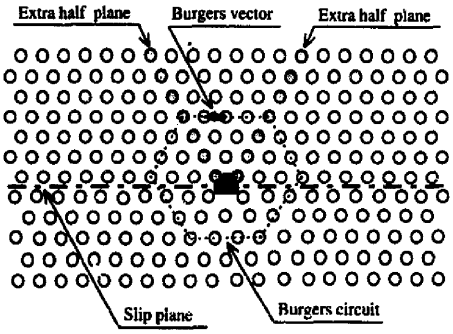

Fig. 3. Determination of edge dislocations.

3. Results

Compared with copper, the bond strength between diamond atoms is much stronger and therefore the distortion of the diamond atomic lattice is negligible. In other words, the diamond can be considered as a rigid body in this study. In the following sections, we shall focus on investigating the atomic lattice deformation of copper.

3.1. Mechanisms of wear

The deformation of the copper specimen has four distinct regimes under sliding. They are the no-wear regime, adhering regime, ploughing regime and cutting regime, as shown in Fig. 4. In the figure, the transition of deformation regimes is characterized by the non-dimensional indentation depth δ, which is defined as d/R and can be viewed, when contact sliding takes place, as a measure of the strain imposed by the diamond asperity.

In the no-wear regime, the atomic lattice of copper is deformed purely elastically. After the diamond asperity slides over, the deformed lattice recovers completely. In this case, sliding does not introduce any wear or initiate any dislocation.

When δ increases and reaches its first critical value, $\delta_c^{(1)}$, adhesion occurs. The atomic bonds of some surface copper atoms are broken by the diamond sliding. These copper atoms then adhere to the asperity surface and move together with it. However, they may form new bonds with other surface atoms of copper and return to the atomic lattice. The above process repeats again and again during sliding, causes a structural

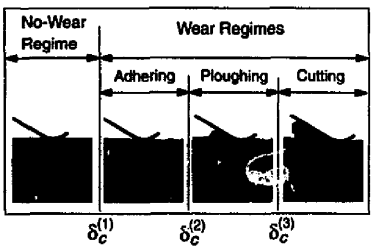

Fig. 4. The transition diagram of deformation regimes. The diamond slides from the right to the left.

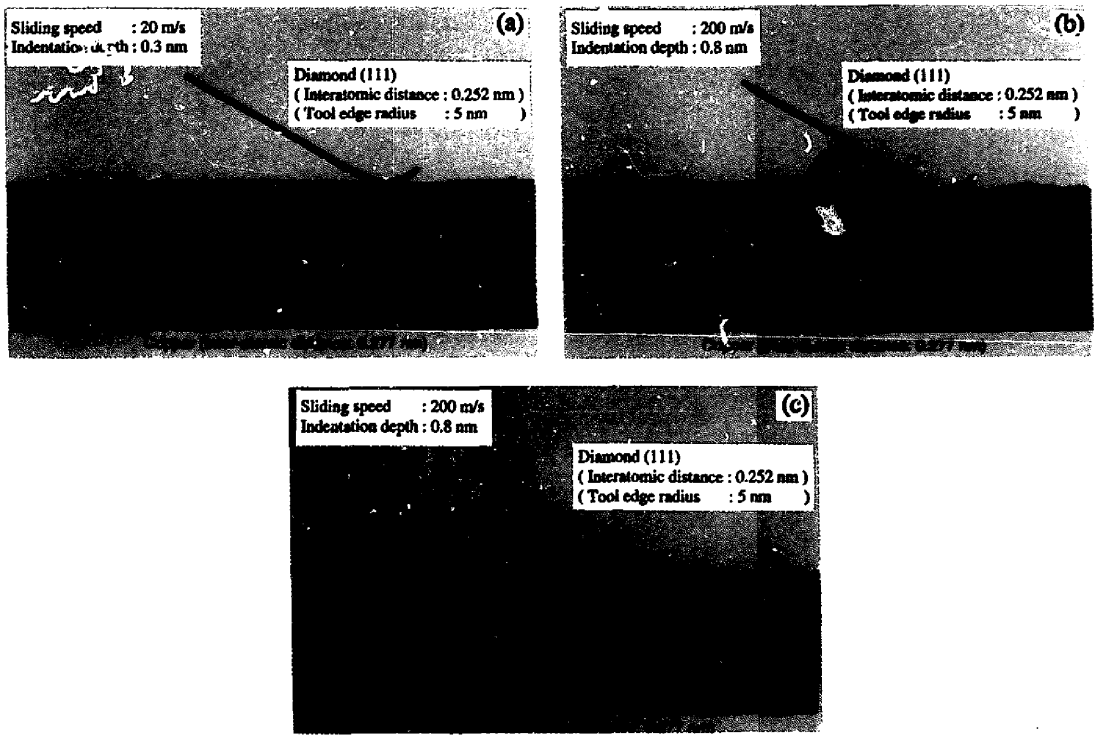

Fig. 5. Distribution of dislocations in the subsurface of copper specimen: (a) adhering regime, (b) ploughing regime, (c) cutting regime. The diamond slides from the right to the left.

change of the copper lattice near the surface, and creates surface roughness of the order of one to three atomic dimensions. In the meantime, some dislocations are also activated in the subsurface, see Fig. 5(a).

If δ increases further to its second critical value, $\delta_c^{(2)}$, the above adhering deformation will be replaced by ploughing (Figs. 4 and 5(b)). An apparent feature of deformation in the stage is that a triangular atom-cluster always exists in front of the leading edge of the diamond asperity and appears as a triangular wave being pushed forward. In this regime, the deformation zone in the subsurface becomes very large and a great number of dislocations are activated. Moreover, the motion of dislocations and their interactions in the subsurface become extremely complex. Grain boundaries can also be generated by ploughing, as shown, for instance, by the continuous orange curve in Fig. 5(b).

When δ reaches its third critical value, $\delta_c^{(3)}$, a new deformation state, cutting, appears, characterized by chip formation. Compared with the ploughing regime, the dimension of the deformation zone during cutting is smaller. Dislocations distribute much more closely to the sliding interface (Fig. 5(c)).

The above figure of deformation regimes and their transition represents the most general case. Under some specific sliding conditions, not all the regimes would appear except the no-wear regime.

For example, if the tip radius of the diamond asperity keeps unchanged but the sliding speed changes, then at lower sliding speeds all the four regimes described above appear. At higher speeds, however, ploughing regime vanishes, see Fig. 6(a). On the other hand, at a given sliding speed, if the tip radius of the asperity is very small, say 1 nm, only no-wear and cutting regimes emerge, as shown in Fig. 6(b). However, with relatively larger tip radii, adhering appears as a transition from no-wear to cutting.

Another important factor that alters the deformation transition is the effect of surface lubrication or contamination. If the sliding interface is chemically clean, $\lambda_1 = \lambda_2 = 1$ in Eq. (1). In this case, as shown in Fig. 6(c), ploughing does not happen at a given sliding speed and tip radius. If the surface is lubricated, $\lambda_1 \leq 1$ with $\lambda_2 \geq 1$, and all the four regimes occur.

It is obvious from Fig. 6 that the no-wear regime exists in a wide range of indentation depths. In addition, a smaller radius, a lower sliding speed, or a better surface lubrication (i.e. smaller λ_1) enlarges the no-wear regime. This highly indicates that a no-wear design of sliding systems may be possible in practice. Moreover, it is important to note that the size of the no-wear regime is a strong function of sliding speed and surface lubrication. Therefore, sliding speed and lubrication should be taken into specific account in an attempt to design no-wear sliding systems.

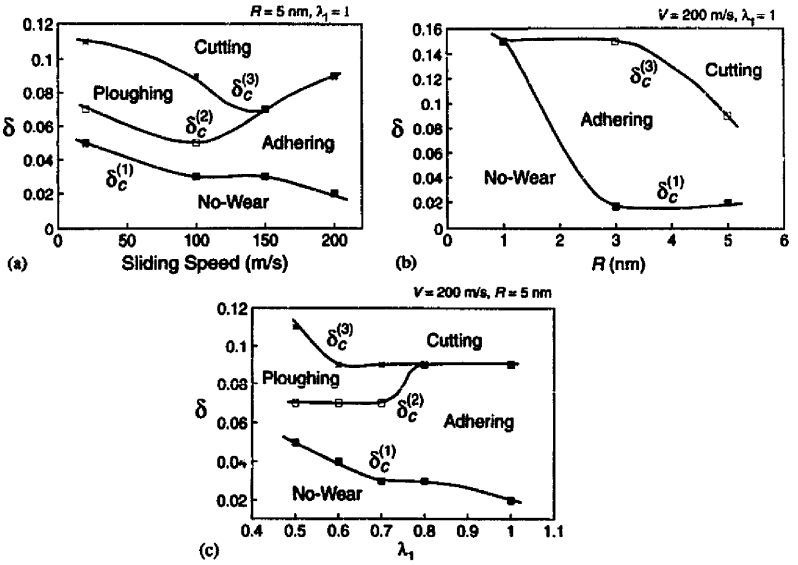

Fig. 6. Regime transition under specific sliding conditions: (a) non-dimensional indentation depth vs. sliding speed, (b) non-dimensional indentation depth vs. tip radius, (c) non-dimensional indentation depth vs. lubrication/contamination.

The formation of various deformation regimes and their transition can be elucidated by the variation of temperature distribution and dislocation motion in the atomic lattice, see Figs. 5 and 7. For instance, a larger indentation depth or a higher sliding speed indicates a higher input sliding energy, greater temperature rise and severe plastic deformation. This

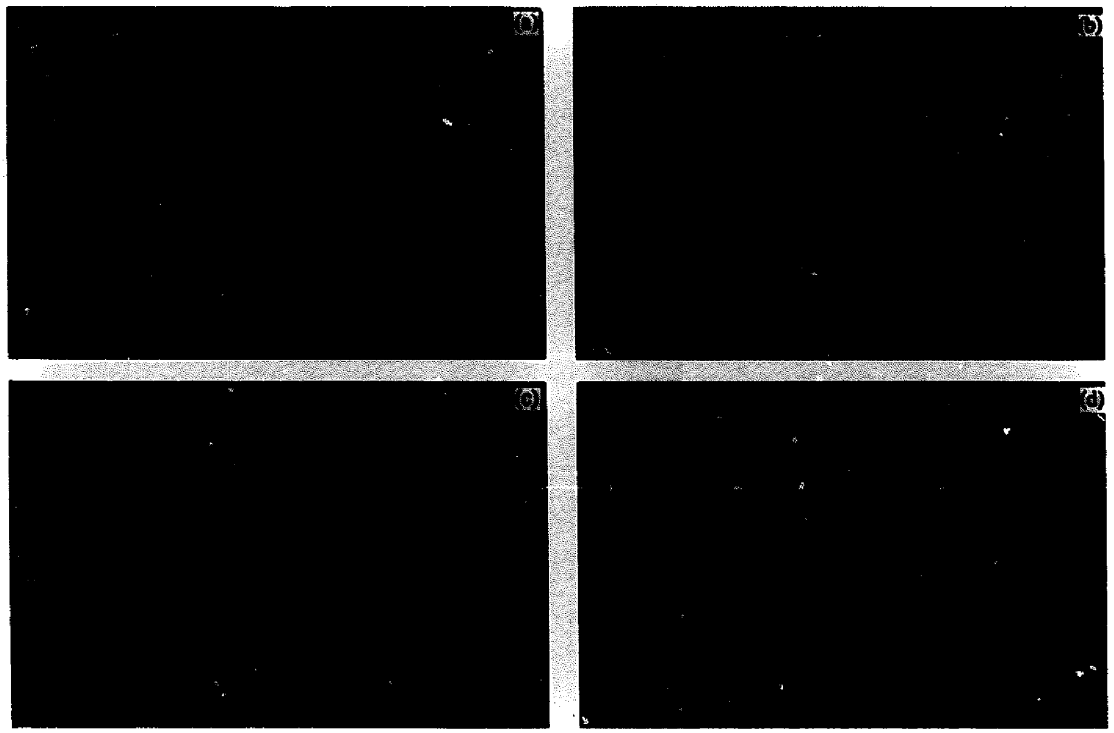

Fig. 7. Temperature distribution in the atomic lattice of copper: (a) no-wear regime, (b) adhering regime, (c) ploughing regime, (d) cutting regime. The diamond slides from the right to the left.

in turn means a higher density of dislocations with more complicated interactions in the deformed atomic lattice. When the non-dimensional indentation depth δ is small, a smaller number of atoms have high temperatures, as shown in Fig. 7(a) and 7(b). Sliding does not cause any considerable temperature rise in the vicinity of the contact zone. With the increase in δ, the number of high temperature atoms increases quickly (Fig. 7(c) and (d)). However, compared with the cutting regime (Fig. 7(d)), the high temperature atoms in the ploughing regime (Fig. 7(c)) distribute in a much wider area. This explains why a ploughing regime has a greater deformation zone and less localized distribution of dislocations (Fig. 5).

3.2. Friction

With the above deformation mechanisms in mind, now let us examine the frictional behaviour of the system. Fig. 8 shows the variation of the conventional friction coefficient, $\mu = |F_x/F_y|$, with the change in δ, where F_x and F_y are respectively the frictional force and normal indentation force during sliding. It is clear that in the cutting regime, F_x is proportional to F_y. In other regimes, however, the behaviour of F_x is complex. Particularly, μ becomes singular at a specific δ in the no-wear regime.

The singularity of μ is understandable if we examine the sliding forces when δ changes. On the atomic scale, as shown in Fig. 9, the normal sliding force F_y always varies from attractive to repulsive. Thus at the transition point ($F_y = 0$), μ is infinite. This also explains why μ varies sharply under different sliding conditions as reported by Refs. [1–7]. All these clearly indicate that the concept of the conventional friction coefficient is no longer meaningful in no-wear, adhering and ploughing regimes.

In non-contact sliding, the only appropriate way to calculate the frictional force is to use Eq. (2). In contact sliding, however, empirical expressions in terms of the contact area can be developed. For example, the following simple formula can be obtained according to the present theoretical analysis,

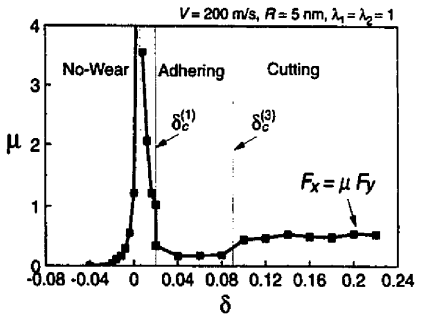

Fig. 8. Variation of friction coefficient.

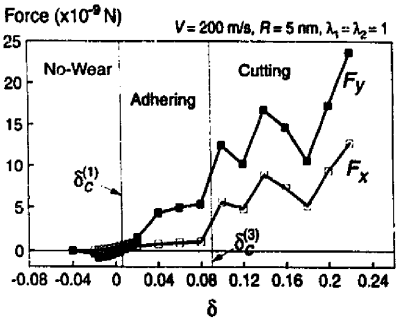

Fig. 9. Variation of sliding forces.

$$F_x = \begin{cases} -\sum_{n=1}^{N_d}\sum_{m=1}^{N_c}\frac{\partial}{\partial x_n}\phi(r_{mn}), & \text{for } L_c = 0 \\ \zeta_1^{II} L_c w_a + \zeta_2^{II}, & \text{for } L_c^{(1)} < L_c \le L_c^{(2)} \\ \zeta_1^{III} L_c w_a + \zeta_2^{III}, & \text{for } L_c > L_c^{(2)} \end{cases} \quad (3)$$

where $\zeta_1^{II} = 409$ MPa, $\zeta_2^{II} = 1.807 \times 10^{-8}$ nN, $\zeta_1^{III} = 4.20$ GPa, $\zeta_2^{III} = -1.899$ nN are constants, N_c is the total number of copper atoms in the model, N_d is the number of diamond atoms, L_c is the atomic contact length and $w_a = 0.226$ nm is the width of an atomic layer of copper in the direction perpendicular to its (111) plane (i.e. the xy-plane in Fig. 1). Eq. (3a) can be derived directly from Eq. (2) by considering that F_x is the resultant force of the atomic forces on all the diamond atoms in the x-direction. Eqs. (3b) and (3c) are empirical expressions by fitting the MD simulation data in Fig. 10. The physical meaning of product $L_c w_a$ in Eq. (3) is the atomic contact area in the present sliding system. As shown by Eq. (3) and Fig. 10, we can see that the frictional behaviour of an atomic sliding system cannot be described by a single formula. There exist two distinct contact sliding zones, zone II ($L_c^{(1)} \le L_c < L_c^{(2)}$) and zone III ($L_c \ge L_c^{(2)}$), where $L_c^{(2)} = 2.216$ nm is the transition boundary from zones II to III, and $L_c^{(1)} = 0.277$ nm is the minimum contact length defined as the distance between two copper atoms in its (111) plane. The transition from non-contact to contact sliding is a sudden change because L_c does not exist below $L_c^{(1)}$. In Fig. 10, zone II reflects the frictional behaviour of the system in the no-wear contact sliding, while zone III shows that in the adhering and ploughing regimes. Thus $L_c^{(2)}$ can be interpreted physically as a critical contact length at which wear takes place. It is easy to obtain according to Fig. 10 that the shearing stress of the present sliding system in the adhering regime, $\tau = F_x/(L_c w_a)$, is in the range 0.7 GPa to 1.5 GPa. With so few dislocations activated in the atomic lattice, it is reasonable to see that τ is close to the theoretical shearing stress of a perfect copper monocrystal, which is $G/2\pi$ (≈ 7.32 GPa) $\ge \tau_{theoretical} \ge G/30$ (≈ 1.53 GPa) [17], where $G \approx 46$ GPa is the shear modulus of copper.

The linear Eqs. (3b) and (3c) are only the rough fittings to the theoretical results. The data scattering in Fig. 10 indi-

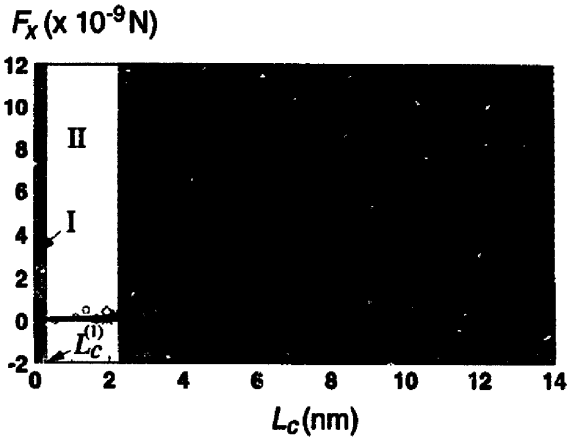

Fig. 10. Relationship between the frictional force and contact length. ×: R=5 nm, V=20 m s^{-1}, λ_1=1. *: R=5 nm, V=100 m s^{-1}, λ_1=1. ★: R=5 nm, V=200 m s^{-1}, λ_1=1. ○: R=1 nm, V=200 m s^{-1}, λ_1=1. ◇: R=5 nm, V=200 m s^{-1}, λ_1=0.5. ■: R=5 nm, V=200 m s^{-1}, λ_1=0.6. +: R=5 nm, V=200 m s^{-1}, λ_1=0.7. □: R=5 nm, V=200 m s^{-1}, λ_1=0.8.

cates that other variables, such as the tip radius of asperity R and sliding speed V, also contribute greatly to friction. In other words, F_x should be a function of not only the contact area $L_c w_a$ but also V, R, and so on.

It is worth noting from Fig. 9 that the frictional force F_x does not vanish under a stable condition even if the system is in non-contact sliding. This is understandable since the interactions between the diamond and copper atoms always exist. In contact sliding with a small indentation depth, F_x remains small until a ploughing or cutting is achieved. Hence, the frictionless sliding mentioned by Belak and Stowers [8] is doubtful. Indeed, in their simulation the indentation motion stopped after 2000 time steps but the 'frictionless motion' ended at the 1000 time step. In that period of time, sliding was still at the very initial transient state. Thus the variation of F_x with the time step of MD simulation does not make sense in terms of the frictional or frictionless sliding. In addition, the normal force variation that they reported is inconsistent with the indentation motion.

3.3. Variation of contact area at high sliding speeds

It is true that the contact area between an asperity and a workpiece is a monotonically increasing function of the indentation load F_y under certain conditions, such as under a low sliding speed and elastic deformation (e.g. Homola et al. [18]). However, it is interesting to point out that this may not be true when sliding at a high speed. In the present study, the contact area $L_c w_a$ varies with L_c only since w_a is a constant. As shown in Fig. 11, at a high sliding speed, 20 m s^{-1} for example, L_c is no longer a monotonically increasing function. This happens, as demonstrated in Fig. 12, because a number of copper atoms (red atoms in the figure) adheres to the diamond surface (black atoms in the figure) during sliding, preventing it from further contact with other copper atoms (e.g. green atoms in the figure) and thus shortening L_c. This, again, indicates that F_x at relatively high sliding speeds must also be a function of other sliding variables rather than the contact area only.

3.4. Similarity and difference between atomic and micro analyses

In the above discussions, we have concentrated on the exploration of deformation mechanisms on the atomic scale.

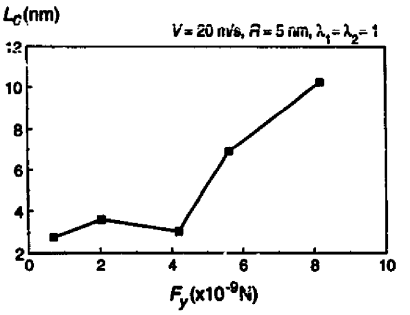

Fig. 11. Variation of the contact length L_c.

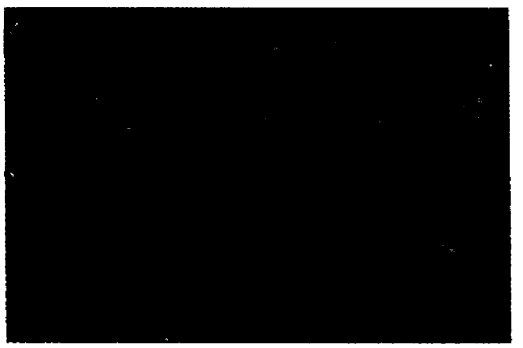

Fig. 12. Mechanism of the contact length shortening at high sliding speeds. The diamond slides from the right to the left.

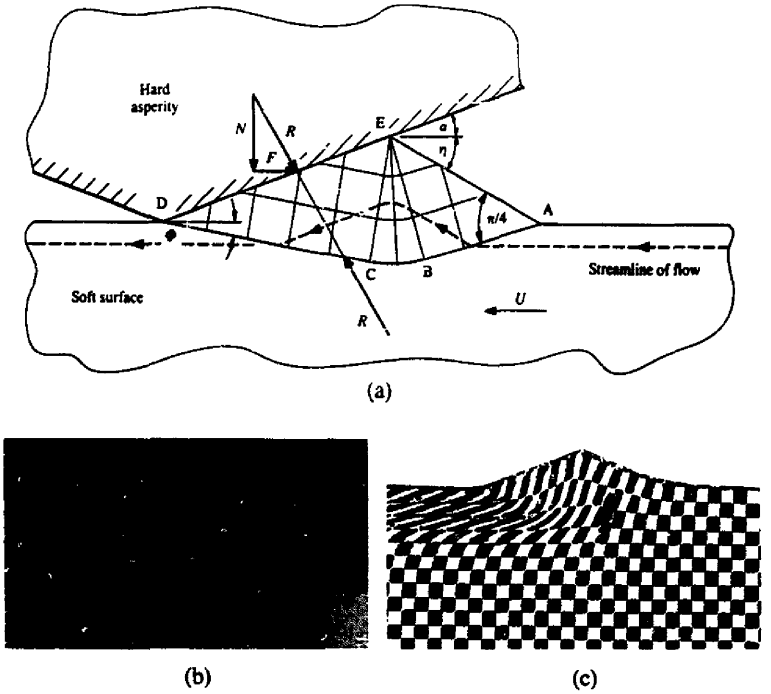

Fig. 13. Deformation mode on the micrometre scale (after Challen and Oxley [19], and Black et al. [20]): (a) the slip-line field of ploughing, (b) the triangular wave during sliding, (c) the distortion of square grids. The indentor slides from the left to the right.

An immediate question to ask is 'Is there any similarity between the deformation on the atomic scale and that on a microscopic scale to which continuum mechanics analysis is still appropriate?'

When the indentation depth is at the micrometre level. Oxley and coworkers [19,20], using the slip-line theory of plasticity, have successfully predicted the frictional behaviour of a sliding system composed of a hard steel asperity and a soft specimen (aluminium–magnesium alloy). Fig. 13(a) shows their slip-line field of the ploughing process. The deformation mode has been approved by relevant experiments, see Fig. 13(b), where the height of the triangular wave is 400 μm, and Fig. 13(c), where the square grid is of 100 μm sides. The distortion of the grids in Fig. 13(c) demonstrates qualitatively the plastic flow in the subsurface of the material. A triangular wave is being pushed forward by the leading edge of the asperity.

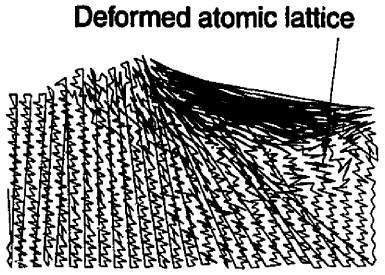

Fig. 14. Distortion of atomic lattice in the ploughing regime at the sliding distance of 300 nm (R=5 nm, λ_1=0.5, V=200 m s^{-1}, δ=0.08). The diamond slides from the right to the left.

As mentioned before, the triangular wave is also a deformation characteristic of the ploughing regime on the atomic scale, see Figs. 4 and 5. In addition, the atomic lattice distortion in the ploughing regime, as shown in Fig. 14, presents a very similar pattern to the experimental observations on the micrometre scale. However, when we examine the details of the dislocation motion and slip-line distribution, see Fig. 5, we can easily find that the deformation mechanisms are different. On the atomic scale, the dislocation motion is mainly discrete and takes place in a large area with its dimension being comparable to the whole deformation zone in the specimen. Thus on the atomic scale, there is not a corresponding slip-line field to that on the micrometre scale. This means that a new theory needs to be developed to bridge the gap between atomic analysis and that using continuum mechanics.

4. Conclusions

In summary, with the aid of the molecular dynamics analysis and modified Morse potential, the present study has acquired the following understandings of wear and friction on the atomic scale.

1. There exist four regimes of deformation in general in an atomic sliding system. They are the no-wear regime which is defect free, adhering regime in which surface atom exchange occurs, ploughing regime which is characterized by a moving triangular atom-cluster, and cutting regime in which material removal takes place.
2. In the cutting regime, the frictional force follows the simple proportional rule $F_x = \mu F_y$. In all the other regimes, the formulae in Eq. (3) apply. However, to describe the frictional behaviour more accurately, the effects of other sliding variables, rather than only the contact area, must be taken into account.
3. The transition between different deformation regimes is governed by indentation depth, sliding speed, asperity geometry and surface lubrication conditions. The most remarkable effects are that a better lubrication, a smaller tip radius, or a smaller sliding speed brings about a greater no-wear regime.
4. The no-wear regime exists in a wide range of indentation depth and thus no-wear designs may be achieved in practice.
5. There does not exist an absolute frictionless contact sliding zone unless the frictional force is assumed to be zero when it is very small.
6. A new theory needs to be developed to bridge the gap between atomic analysis and that using continuum mechanics.
7. A modified Morse potential function has been proposed for studying qualitatively the effect of surface contamination.

5. Notation

D cohesive energy between two atoms, see Fig. 2
d indentation depth, defined as the overlap between the tip of the diamond asperity and the upper surface of the copper specimen, see Fig. 1
F sliding force
L_c atomic contact length between the diamond and copper surfaces
R tip radius of the diamond asperity, defined as the radius of the envelope of centres of the surface atoms
r interatomic separation, see Fig. 2
r_0 equilibrium separation between two atoms at which the net potential energy minimizes, see Fig. 2
T temperature
V sliding speed of the diamond asperity
w_a the width of an atomic layer of copper in the direction perpendicular to its (111) plane, 0.226 nm
δ non-dimensional indentation depth, defined as d/R
λ_1, λ_2 non-dimensional parameters in the modified Morse potential in Eq. (1), indicating the interaction strength change between copper and diamond atoms
ϕ modified Morse interatomic potential, defined by Eq. (1), see also Fig. 2

Subscripts

x in the direction of x-axis, i.e. the sliding direction, see Fig. 1
y in the direction of y-axis, i.e. the direction normal to the sliding direction, see Fig. 1

Acknowledgements

The authors are grateful to Professor K.L. Johnson (University of Cambridge, UK) and Professor P.L.B. Oxley (University of New South Wales, Australia) for their invaluable comments. The continuous support from the Australian Research Council through its ARC Large Grant Scheme is appreciated.

References

[1] C.M. Mate, G.M. McClelland, R. Erlandsson, S. Chiang, Phys. Rev. Lett. 59 (1987) 1942–1945.
[2] R. Kaneko, K. Nonoka, K. Yasuda, J. Vac. Sci. Technol. A 6 (1988) 291–292.
[3] P. Bak, Res. Prog. Phys. 45 (1982) 587–629.
[4] W. Zhong, D. Tomanek, Phys. Rev. Lett. 64 (1990) 3054–3057.
[5] G.M. McClelland, in: H.J. Kreuzer, M. Grunze (eds.), Adhesion and Friction, Springer-Verlag, Berlin, 1989, pp. 1–16.
[6] J.B. Sokoloff, Surf. Sci. 144 (1984) 267–272.
[7] U. Landman,W.-E. Luedtke, M.W. Ribarsky, J. Vac. Sci. Technol. 47 (1989) 2829–2839.
[8] J. Belak, I.F. Stowers, in: I.L. Singer, H.M. Pollock (eds.), Fundamentals of Friction: Macroscopic and Microscopic Processes, Kluwer, Dordrecht, 1992, pp. 511–520.
[9] A.M. Homola, Wear 136 (1990) 65–83.
[10] F.P. Bowden, D. Tabor, Friction and Lubrication, Methuen, London, 1967.
[11] K.L. Johnson, K. Kendall, A.D. Roberts, Proc. R. Soc. London Ser. A 324 (1971) 301–313.
[12] W. Hoover, Molecular Dynamics, Springer-Verlag, Berlin, 1986.
[13] N. Ikawa, S. Shimada, H. Tanaka, G. Ohmoei, Ann. CIRP 40 (1991) 551–554.
[14] S. Shimada, N. Ikawa, H. Tanaka, J. Uchikoshi, Ann. CIRP 43 (1994) 51–54.
[15] H. Tanaka, L.C. Zhang, in: N. Narutaki et al. (eds.), Progress of Cutting and Grinding, Japan Society for Precision Engineering, Osaka, 1996, pp. 262–266.
[16] L.C. Zhang, H. Tanaka, Some essential considerations in molecular dynamics modelling of sliding systems, in preparation.
[17] T.H. Courtney, Mechanical Behaviour of Metals, McGraw-Hill, Singapore, 1990, pp. 81–83.
[18] A.M. Homola, J.N. Israelachvili, M.-L. Gee, P.M. McGuiggan, Trans ASME J. Tribol. 111 (1989) 675–682.
[19] J.M. Challen, P.L.B. Oxley, Wear 53 (1979) 229–243.
[20] A.J. Black, E.M. Kopalinsky, P.L.B. Oxley, IMechE J. Mech. Eng. Sci. C207 (1993) 335–353.

Biographies

L.C. Zhang received his PhD degree from Peking University in 1988. He is currently a senior lecturer at the University of Sydney, Department of Mechanical and Mechatronic Engineering, prior to which he worked at the Mechanical Engineering Laboratory, Japan, University of Cambridge, UK, and Zhejiang University, China. He is teaching and researching in the field of solid mechanics with particular interest in the area of materials removal mechanisms of ultra-precision machining processes, wear and friction, characterization of engineering materials, development of numerical methods and sheet metal forming.

H. Tanaka received his PhD degree from Osaka University in 1993. He is now a research associate at the University of Sydney, Department of Mechanical and Mechatronic Engineering. Before he came to Australia, he worked at the R&D Section for Precision Technology of SONY Corporation, Tokyo, Japan. His research interest is in the area of ultra-precision machining.